Biomedicine & Pharmacotherapy 98 (2018) 406–415

Contents lists available at ScienceDirect

Biomedicine & Pharmacotherapy

journal homepage: www.elsevier.com/locate/biopha

Effects of estrogen status in osteocyte autophagy and its relation to osteocyte viability in alveolar process of ovariectomized rats

Rinaldo Florencio-Silva[a], Gisela R.S. Sasso[b], Estela Sasso-Cerri[c], Manuel J. Simões[a], Paulo S. Cerri[c,*]

[a] Universidade Federal de São Paulo - UNIFESP, Escola Paulista de Medicina – EPM, Departamento de Morfologia e Genética, Disciplina de Histologia e Biologia Estrutural, São Paulo, SP, Brazil
[b] Universidade Federal de São Paulo - UNIFESP, Escola Paulista de Medicina – EPM, Departmento de Ginecologia, São Paulo, SP, Brazil
[c] São Paulo State University (UNESP), School of Dentistry, Araraquara – Laboratory of Histology and Embryology, Araraquara, SP, Brazil

ARTICLE INFO

Keywords:
Osteocytes
Autophagy
Apoptosis
Estrogen
Alveolar process

ABSTRACT

Estrogen maintains osteocyte viability, whereas its deficiency induces osteocyte apoptosis. As autophagy is important for osteocyte viability, we hypothesized whether the anti-apoptotic effect of estrogen is related to autophagy in osteocytes. Thirty adult female rats were sham-operated (SHAM) or ovariectomized (OVX). After three weeks, twelve rats of SHAM and OVX groups were killed before treatment (basal period), whereas the remaining rats received estrogen (OVXE) or vehicle (OVX) for 45 days. Fragments of maxilla containing alveolar process of the first molars were embedded in paraffin or Araldite. Paraffin-sections were stained with hematoxylin/eosin for histomorphometry, or subjected to the silver impregnation method for morphological analysis of osteocyte cytoplasmic processes. Autophagy was analyzed by immunohistochemical detections of beclin-1, MAP-LC3α and p62, whereas apoptosis was evaluated by immunohistochemical detections of cleaved caspase-3 and BAX, TUNEL (Terminal deoxynucleotidyl transferase dUTP nick end labeling) method and by ultrastructural analysis. Araldite-semithin sections were subjected to the Sudan-black method for detection of lipids. OVX-basal group showed high frequency of caspase-3-, TUNEL- and p62-positive osteocytes accompanied with low frequency of beclin-1- and MAP-LC3α-positive osteocytes. At 45 days, OVXE group exhibited higher number of osteocytes, higher frequency of beclin-1- and MAP-LC3α-positive osteocytes, and lower frequency of caspase-3, BAX-, TUNEL- and p62-positive osteocytes than OVX group. Significant reduction in bone area was observed in the OVX compared to OVXE and SHAM groups. The highest frequency of Sudan-Black-positive osteocytes and osteocytes with scarce cytoplasmic processes, or showing apoptotic features were mainly observed in OVX groups. Our results indicate that estrogen deficiency decreases autophagy and increases apoptosis, whereas estrogen replacement enhances osteocyte viability by inhibiting apoptosis and maintaining autophagy in alveolar process osteocytes. These results suggest that the anti-apoptotic effect of estrogen may be, at least in part, related to autophagy regulation in osteocytes.

1. Introduction

Osteocytes, the most abundant bone cell type, play essential roles for the maintenance of bone homeostasis by acting as mechanosensors and orchestrators of the bone remodeling process [1–3]. As osteocytes are long-living cells encased in mineralized bone matrix, they are located in an environment more susceptible to hypoxia, nutrient deprivation and to the accumulation of oxidative stress [4]. In addition, increasing number of studies has shown that autophagy plays essential role for osteocyte survival [5–8].

Autophagy is a programmed cell survival mechanism whereby unnecessary cellular components such as malfunctioning proteins and organelles are targeted to the lysosomes for degradation. The molecules resulting from this degradation are converted into substrates for energy production when nutrients are limiting [9]. Basal autophagy occurs in all cell types, but it can be induced by factors that cause cell stress including nutrient deprivation, hypoxia and increased oxidative stress [10,11]. The process of autophagy begins with the formation and nucleation of the phagophore, a membrane that elongate engulfing non-functional cytoplasmic material to form the autophagosomes [9].

* Corresponding author at: UNESP - São Paulo State University, Araraquara Dental School Rua Humaitá, 1680, Centro, CEP 14801–903, Araraquara, SP, Department of Morphology - Laboratory of Histology and Embryology, Brazil.
E-mail address: pcerri@foar.unesp.br (P.S. Cerri).

https://doi.org/10.1016/j.biopha.2017.12.089
Received 3 October 2017; Received in revised form 5 December 2017; Accepted 18 December 2017

Beclin-1 and the microtubule-associated protein 1A/1B-light chain (MAP LC3) are autophagic proteins essential for phagophore nucleation and elongation, respectively [11].

There are three human genes that encode highly homologous MAP LC3 proteins (MAP LC3α, MAP LC3β, and MAP LC3γ), two of which (MAP LC3α and MAP LC3β) are conserved in rodents [12]. MAP LC3α, MAP LC3β, and MAP LC3γ are either cytosolic (MAP LC3I) or membrane associated (MAP LC3II) proteins. MAP LC3α and MAP LC3β are essential for autophagosome formation; during phagophore elongation, the cytosolic form of LC3 (MAP LC3-I) is conjugated to phosphatidylethanolamine to form LC3-phosphatidylethanolamine conjugate (MAP LC3-II), which is recruited to the autophagosomal membrane. Specific malfunctioning proteins can also be selectively directed to autophagosomes by the sequestosome 1 (SQSTM1), also known as p62 protein, which binds to ubiquitinated non-functional proteins and targeting them to autophagosomes for lysosome degradation. p62 is also degraded in this process, then acting as a specific autophagosome substrate that indicates the levels of autophagic flux in cells [13].

In recent years, studies have shown that autophagy plays important roles for the maintenance of bone homeostasis, and its dysregulation has been related to bone loss and osteoporosis [18],14–17]. It has been demonstrated that suppression of ATG7 (autophagy related 7), an essential gene for autophagy, in mice osteocytes promotes a marked increase in oxidative stress and bone loss [18]. Also, an age-related reduction in the autophagic flux in osteocytes was correlated to bone loss and osteoporosis in senile rats [19]. More recently, it has been demonstrated that rapamycin, an inductor of autophagy, reduces the severity of age-related trabecular bone loss by activating autophagy in osteocytes of old male rats [20]. All these studies strongly indicate that autophagy is essential for osteocyte viability and bone homeostasis.

On the other hand, estrogen plays essential role for the maintenance of bone homeostasis by inhibiting both excessive bone resorption and osteoblast/osteocyte apoptosis [21–23]. It has been shown that the pro-survival effect of estrogen is in part related to autophagy levels in bone cells [24,25]. Estrogen added to osteoblasts in culture induces autophagy and reduces apoptosis, suggesting that this hormone increases osteoblast survival by autophagy induction [24]. In tibias of ovariectomized rats, estrogen deficiency increased oxidative stress, which then induced autophagy in osteoblasts and osteocytes, whereas estrogen replacement counteracted these effects [25].

It has widely been demonstrated that estrogen deficiency induces bone loss not only in the vertebrae and long bones, but in bone surrounding teeth as well [26–29]. However, despite similarities, it is known that long and jaw bones display different osteogenic and osteoclastogenic potentials, and can also respond differently to mechanical loading, homeostatic regulatory signals and estrogen deficiency [30–33]. Despite it has been reported that estrogen status regulates bone cell autophagy in vitro and in long bones of OVX rats, its effects on osteocyte autophagy in jaw bones is poorly understood.

Thus, in this study we hypothesized whether the protective effect of estrogen is related to autophagy incidence in alveolar process osteocytes, using ovariectomized rats as an estrogen-deficient in vivo model.

2. Material and methods

2.1. Animals and experimental protocol

Thirty female Wistar rats (*Rattus norvegicus albinus*) aged 4 months were maintained in a room with controlled temperature (23 ± 2 °C) and standard 12-h light/dark cycle, with food and water *ad libitum*. The protocol of this study followed the national guidelines for laboratory animal care and was approved by the Ethical Committee for Animal Research of Federal University of São Paulo (UNIFESP/EPM).

After one week of adaptation period, the animals were anaesthetized with an intraperitoneal injection of 10% ketamine hydrochloride (0.08 mL/100 g b.w.) combined with 2% xylazine hydrochloride (0.04 mL/100 g b.w.) and then SHAM-operated (SHAM) or ovariectomized (OVX). Ovariectomy was followed by a resting period of twenty-one days to ensure estrogen depletion and recovery from surgery stress, as previously reported [29,34].

Twenty-one days after surgery, vaginal smears were obtained once a day during five consecutive days in all animals; only the SHAM rats that showed regular estrous cycle and the OVX rats that were in permanent anestrous followed in the experiment. At this point, 6 SHAM and 6 OVX rats were euthanized (as described below) and used as basal control groups (basal period). The other animals received subcutaneous injections of estrogen (OVXE) (diethylstilbestrol, Sigma-Aldrich Co. LLC, Brazil), dissolved in corn oil, at the dose of 30 μg/kg body weight [35], or received only corn oil as vehicle solution (SHAM and OVX groups), for 45 consecutive days (n = 6 rats for each group). The analysis was performed after 45 days to ensure significant bone loss in the alveolar process in the OVX group, as previously described in this animal model [30].

After treatment, the animals were anaesthetized as previously described and blood samples (2 mL each) were collected by cardiac puncture (BD Vacutainer® Blood Collection Tubes, SST II Plus, BD Biosciences). The blood samples were centrifuged and the serum stored at -80 °C for serum estradiol measurement. The animals were euthanized by whole body fixation via transcardial perfusion with saline followed by a fixative solution of 4% formaldehyde (prepared from paraformaldehyde) in 0.1 M sodium phosphate buffer solution, pH 7.2. Subsequently, the fragments of maxilla containing alveolar process surrounding the first molars were removed and immediately immersed in the fixative solution.

2.2. Estradiol measurement

Serum estradiol concentration was measured by an electrochemiluminescence immunoassay using a calibrated automatic counter (Cobas e601/Roche Diagnostic, Mannheim Germany). An estradiol kit containing rabbit polyclonal biotinylated antibody specific for estradiol detection in rats and humans (Roche Cobas Estradiol II assay/03000079, Mannheim, Germany) was used. The linear range of the assay was 5 pg/mL to 3000 pg/mL and the coefficient of variation intra-assay was 3.3%. The samples were dosed in duplicate and values below the limit of detection (< 5 pg/mL) were not detected by the assay. The analyses were performed in the Central Laboratory of São Paulo Hospital (HSP), SP, Brazil.

2.3. Histological processing

Fragments of the right maxilla were immersed for 48 h at room temperature in 4% formaldehyde buffered pH 7.2 with 0.1 M sodium phosphate. After decalcification for 60 days in a solution of 7% EDTA (ethylenediaminetetraacetic acid) that contained 0.5% formaldehyde in 0.1 M sodium phosphate buffer at pH 7.2, the fragments were dehydrated and embedded in paraffin. Sagittal sections (6 μm thick) were stained with hematoxylin and eosin (HE), and bone area of the alveolar process situated between the first molar roots was measured. The number of osteocytes in the alveolar process was also estimated. Some sections were subjected to the silver impregnation method for morphological analysis of osteocyte cytoplasmic processes. Sections were also adhered to silanized slides and subjected to TUNEL (Terminal deoxynucleotidyl transferase dUTP nick end labeling) and immunohistochemical reactions.

2.4. Interradicular bone area

The bone area of the alveolar process situated between the first molar roots was estimated using a software of image analysis (Axionvision 4.2 REL, Carl Zeiss) coupled with a light microscope (Axiolab 2.0, Carl Zeiss). At a magnification of ×40, two images/

animal (with a minimum distance of 100 µm between sections) of the alveolar process were captured. In each image, a standardized area of approximately 1 mm^2 was demarcated. Then, only bone tissue in this area was delimited. The obtained data were then quantified and expressed as percentage/total area in each image. From the percentage of bone area in each image, an average percentage for each animal and then for each group was obtained. The abbreviations of the histomorphometrical parameters were based on the nomenclature standardized by the American Society for Bone and Mineral Research [36].

2.5. Numerical density of osteocytes

Two non-serial HE-stained sections from each animal were used and, in each section, five standardized fields were captured totaling ten fields per animal. The images were captured using a camera (DP-71, Olympus) attached to a light microscope (Olympus, BX-51) at ×40 magnification. Using an image analysis system (Image Pro-express 6.0, Olympus), the number of osteocytes (N.Ot/mm^2) in the alveolar process located between the first molar roots was computed in a standardized area (0.09 mm^2).

2.6. Morphological analysis of osteocyte cytoplasmic processes by silver impregnation

Sections were subjected to the Silver impregnation method to identify osteocyte cytoplasmic processes, as previously described [37]. Briefly, deparaffinized and hydrated sections were immersed in milliQ water for 10 min. Subsequently, the sections were incubated in a 50% aqueous silver nitrate solution containing 1% formic acid and 2% agar solution, in a humidified chamber at 40 °C for 20 min. After washing in milliQ water for 10 min, the sections were dehydrated and then mounted in Canada balsam mounting medium (Synth, São Paulo, Brazil).

2.7. Terminal deoxynucleotidyl transferase dUTP nick end labeling (TUNEL method) and frequency of TUNEL-positive osteocytes

Sections of the upper maxilla containing the alveolar process of the first molars were subjected to the TUNEL method for detection of DNA breaks [38]. The protocol of the TUNEL method was performed using the Apop-Tag® Peroxidase In Situ Apoptosis Detection Kit (Millipore; Temecula, CA, USA), as previously described [39]. The reaction was revealed with 3,3-diaminobenzidine (DAB, DAKO Corporation, USA) and the sections were counterstained with hematoxylin. Sections of involuting mammary gland provided by the manufacturer of the kit were used as positive control. As negative control, the sections containing alveolar process were incubated in a Terminal deoxynucleotidyl transferase (TdT) enzyme-free solution.

In each section, eight fields of the interradicular alveolar process were captured using a camera (DP-71, Olympus) attached to a light microscope (Olympus, BX-51), at ×100 magnification. Using an image analysis system (Image Pro-express 6.0, Olympus), the total number of osteocytes was computed in each standardized area. The number of TUNEL-positive osteocytes was counted and the frequency (in percentage) of TUNEL-positive osteocytes was obtained.

2.8. Immunohistochemical reactions and frequency of immunolabeled osteocytes

Immunohistochemical reactions for detection of beclin-1, MAP LC3α and p62, and for detection of cleaved caspase-3 and BAX were carried out to evaluate autophagy [40] and apoptosis [39,41], respectively.

Deparaffinized sections were immersed in 3% hydrogen peroxide for 20 min to block the endogenous peroxidase. For antigen retrieval, the sections were immersed in 0.001 M sodium citrate buffer pH 6.0 and maintained at 90–94 °C, in a vapor cooker, for 40 min. After cooling, the slides were washed in 50 mM PBS at pH 7.2 and incubated with 5% skimmed milk at room temperature. The sections were incubated in a humidified chamber at 4 °C overnight with the following primary antibodies: 1-) rabbit anti-cleaved caspase-3 polyclonal antibody (Millipore®, SP, Brasil), diluted 1:100; 2-), rabbit anti-BAX monoclonal antibody (Spring, Bioscience, CA, USA), diluted 1:100; 3-), rabbit anti-beclin-1 polyclonal antibody (Santa Cruz®, CA, USA), diluted 1:600; 4-), rabbit anti-MAP LC3α polyclonal antibody (Santa Cruz®, CA, USA), diluted 1:200; 5-), or mouse anti-p62 monoclonal antibody (Santa Cruz®, CA, USA), diluted 1:100. After washing in PBS, the immunoreactions were amplified using a Labeled Streptavidin-Biotin kit (LSAB-plus kit; DAKO Corporation, USA). Peroxidase activity was revealed by 3,3′-diaminobenzidine (DAB, DAKO Corporation, USA) and the sections were counterstained with Carazzi's hematoxylin. For negative controls, the step of incubation in primary antibodies was replaced by the incubation in non-immune serum (Sigma-Aldrich, Germany).

Each immunohistochemical reaction was performed in two non-serial sections, totaling twelve sections per group. In each section, eight fields (standardized area) of the interradicular alveolar process of the first molar were captured using a camera (DP-71, Olympus) attached to a light microscope (Olympus, BX-51), at ×100 magnification. In each standardized area of the interradicular alveolar process, the total number of osteocytes and the number of immunolabeled osteocytes for each immunoreaction was computed. Thus, the frequency was calculated by number of immunolabeled osteocytes in relation to the total number of osteocytes in each standardized area of the alveolar process. The frequency, expressed as percentage (%), of immunostained osteocytes for each immunoreaction was then obtained.

2.9. Transmission electron microscopy (TEM)

Fragments of maxilla containing alveolar process of the first molars were fixed for 16 h in a solution containing 4% glutaraldehyde and 4% formaldehyde in 0.1 M sodium cacodylate buffer, pH 7.2. After decalcification in a solution of 7% EDTA in 0.1 M sodium cacodylate buffer at pH 7.2, the fragments were immersed in cacodylate-buffered 1% osmium tetroxide at pH 7.2 for 1 h. Subsequently, the fragments were washed in distilled water and immersed in 2% aqueous uranyl acetate for 2 h. After washing, the fragments were dehydrated in graded concentrations of ethanol, treated with propylene oxide and then embedded in Araldite® (Electron Microscopy Sciences) [39].

Semithin sections stained by 1% methylene blue/azure II solution were examined under a light microscope, and suitable regions were carefully selected for trimming of the blocks. Ultrathin sections were collected onto cooper grids and stained with alcoholic 2% uranyl acetate and lead citrate, and examined in a transmission electron microscope (Tecnai G2 Spirit, FEI Company).

2.10. Sudan Black histochemistry for detection of lipid droplets

Four non-serial semithin sections of each specimen (three rats per group, totaling 12 sections per group) were subjected to the Sudan Black method for the lipid droplets detection in osteocytes [42]. Four fields (standardized area) in each section (totaling 48 fields per group) were captured by a camera (DP-71, Olympus) attached to a light microscope (Olympus, BX-51), at ×100 magnification.

Using an image analysis system (Image Pro-express 6.0, Olympus), the total number of osteocytes and the number of osteocytes exhibiting Sudan-positive inclusions in their cytoplasm was counted in each standardized area of the interradicular alveolar process. The percentage of osteocytes exhibiting Sudan Black-positive inclusions was calculated.

Table 1
Mean and standard deviation of the estradiol serum levels (pg/mL).

Time points	SHAM	OVX	OVXE
Basal	21.02 ± 7.17	< 5	
45 days	26.10 ± 21.26	< 5	701.70 ± 78.37*

* p < .05 (OVXE > SHAM). Serum levels below 5 pg/mL were not detected by the assay.

2.11. Statistical analysis

Data were expressed as means ± standard deviation (SD). The groups were compared using one-way analysis of variance (ANOVA), followed by Tukey's multiple comparison test to evaluate differences among groups; tests for variance homogeneity and normal distribution were also applied. A two-way analysis of variance, followed by the Bonferroni post hoc test was performed to evaluate two variables (time and treatment) between the SHAM and OVX groups, at both periods analyzed (basal and 45 days). Statistical analyses were performed using the GraphPad Prism 5 software (GraphPad Software, Inc., San Diego, CA) and the significance level was established at $p \leq .05$.

3. Results

3.1. Estradiol serum levels

According to the Table 1, the serum levels of estradiol were significantly higher ($p < .05$) in the SHAM and OVXE than in OVX group. Moreover, the serum levels of estradiol in the OVX groups were below the detection limit of the assay (Table 1).

3.2. Morphological and histomorphometrical findings

The alveolar process between the roots of first molars (Fig. 1A) exhibited bone cavities filled with bone marrow (Fig. 1B). Osteocyte profiles were frequently observed inside the lacunae in the alveolar process (Fig. 1C–E). In the OVX group, osteocytes exhibited scarce cytoplasmic processes whereas in the SHAM and OVXE groups, numerous cytoplasmic processes were observed in the osteocytes (Fig. 1F–H).

The quantitative analyses revealed significant reduction ($p < .05$) of the interradicular bone area in the OVX group compared with the SHAM and OVXE groups at 45 days (Fig. 1I). The number of osteocytes was significantly lower ($p < .05$) in the OVX than the SHAM group in the basal period. At 45 days, the number of osteocytes was significantly higher ($p < .05$) in the OVXE than in OVX group, whereas significant differences between OVXE and SHAM groups were not detected (Fig. 1J).

3.3. Osteocyte cell death

In all groups, osteocytes exhibiting immunostained cytoplasm (brown-yellow color) for BAX (Fig. 2A–C) and cleaved caspase-3 (Fig. 2E–G) were found in the bone of alveolar process. Some TUNEL-positive osteocytes were also observed (Fig. 2I–K). In the sections used as negative controls, no immunolabeled cells were found (Fig. 2D and H). The mammary gland sections used as positive control showed numerous TUNEL-positive cells (data not illustrated), while the sections incubated in the TdT enzyme-free medium were negative (Fig. 2L).

The ultrastructural analysis of the alveolar process revealed osteocytes with cytoplasmic processes extending from the osteocyte cell body towards the bone canaliculi (Fig. 2M–O). Moreover, some osteocytes exhibiting scarce cytoplasm with few organelles and showing condensed chromatin filling almost all nucleus were observed, mainly in the OVX groups (Fig. 2N).

3.4. Frequency of BAX-, caspase-3-immunolabeled and TUNEL-positive osteocytes

Significant differences in the frequency of BAX-positive osteocytes were not detected between SHAM and OVX groups in the basal period. After 45 days, the frequency of BAX-positive osteocytes was significantly higher ($p < .05$) in the OVX group than in SHAM and OVXE groups, whereas significant difference was not observed between OVXE and SHAM groups (Fig. 2P).

A significant increase ($p < .05$) in the frequency of caspase-3-immunolabeled osteocytes was observed in the OVX compared to SHAM group, in the basal period. At 45 days, the frequency of caspase-3-immunolabeled osteocytes was significantly lower ($p < .05$) in the OVXE group than in OVX group. Significant differences were not detected between OVXE and SHAM groups at 45 days. From basal period to 45 days, a significant increase ($p < .05$) in the frequency of immunolabeled osteocytes in the rats of OVX groups was found (Fig. 2Q).

According to the Fig. 2R, the quantitative analysis of TUNEL method revealed a significant increase ($p < .05$) in the frequency of TUNEL-positive osteocytes in the alveolar process of OVX group compared with SHAM group, in the basal period and after 45 days. At 45 days, significant differences were not observed between OVXE and SHAM groups.

3.5. Autophagy mediators: frequency of beclin-1-, MAP LC3α- and p62-immunolabeled osteocytes

In all the groups, the alveolar process showed numerous beclin-1-immunolabeled osteocytes (around 70–90%) in the periods examined (Fig. 3A–C). On the other hand, only few MAP LC3α- and p62-immunolabeled osteocytes were observed in the alveolar process (Fig. 3D–I). In the sections used as negative controls, no immunolabeled cells were found (3J-3L).

In the basal period, a significant reduction ($p < .05$) in the frequency of immunolabeled osteocytes for beclin-1 and MAP LC3α was observed in the OVX compared to SHAM group (Fig. 3M and N). At 45 days, the frequency of beclin-1- and MAP LC3α-immunolabeled osteocytes was significantly lower ($p < .05$) in OVX group than in SHAM and OVXE groups (Fig. 3M and N). In contrast, a significant increase ($p < .05$) in the incidence of p62-immunolabeled osteocytes was observed in the OVX than in OVXE and SHAM groups at 45 days. From basal period to 45 days, a significant increase ($p < .05$) in the frequency of p62-positive osteocytes (Fig. 3O) was detected in the OVX group. Moreover, significant differences in the frequency of beclin-1-, MAP LC3α- and p62-immunolabeled osteocytes were not observed between OVXE and SHAM groups at 45 days (Fig. 3M–O).

3.6. Lipid droplets in osteocytes

Semithin sections submitted to the Sudan Black B method showed some Sudan Black-positive inclusions (lipid droplets) in the osteocytes of all the groups (Fig. 4A–D). The quantitative analysis showed that the OVX group presented a significant increase ($p < .05$) in the frequency of osteocytes containing lipid droplets compared with SHAM group in the basal period.

From basal period to 45 days, a significant increase ($p < .05$) in the frequency of these osteocytes was observed in the SHAM and OVX groups. At 45 days, the highest frequency of osteocytes with lipid droplets was found in the OVX group; significant differences were not observed between OVXE and SHAM groups (Fig. 4E).

The ultrastructural analysis revealed that these lipid droplets exhibited variable shape and size and were present in the osteocytes of all the groups (Fig. 4F–K). Some of these osteocytes showed nucleus with irregular masses of condensed chromatin (Fig. 4G).

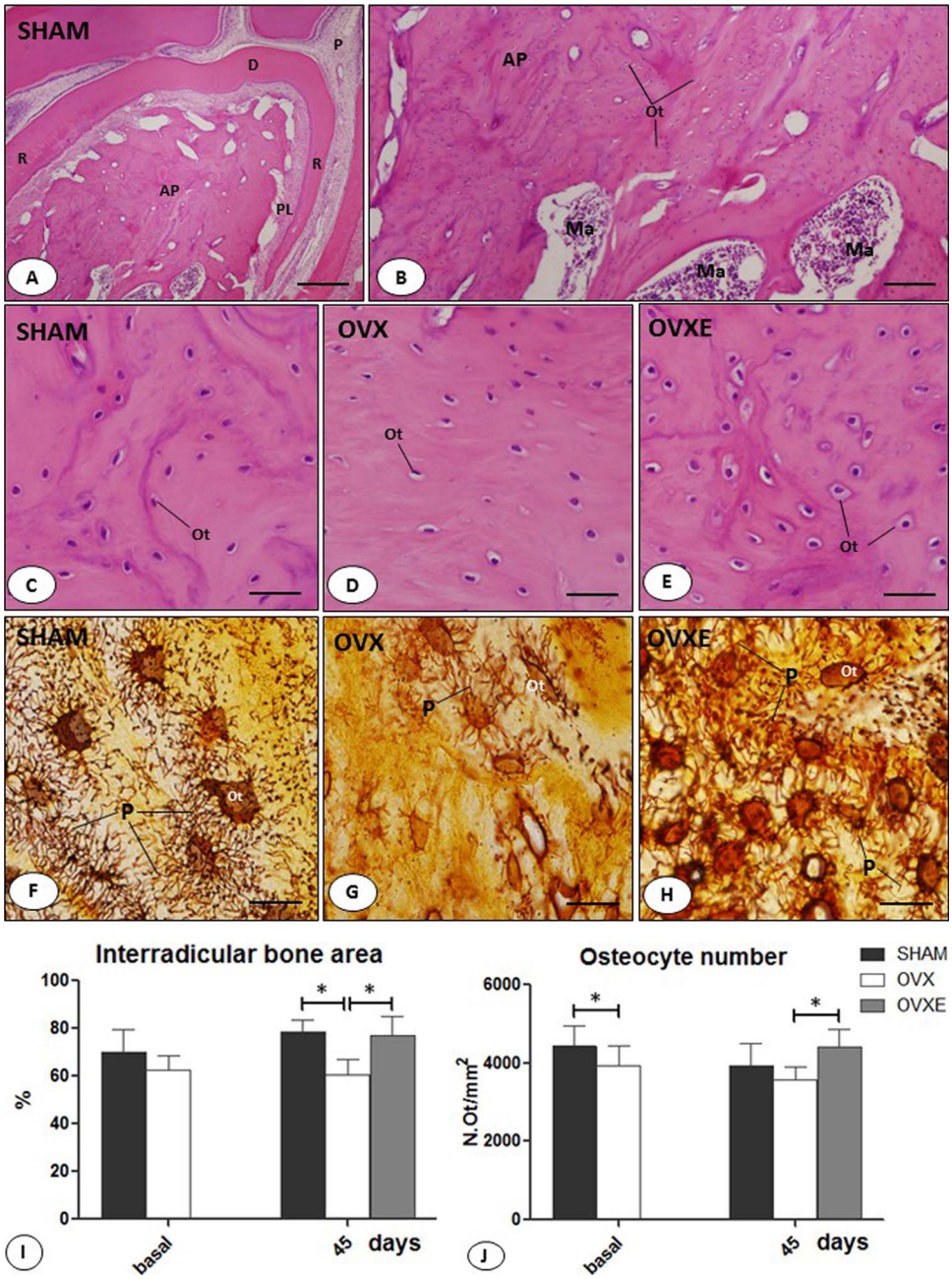

Fig. 1. A–H – Light micrographs of sections of maxilla showing portions of the interradicular alveolar process of first molars from groups at 45 days. In the **A–E**, the sections were stained with HE. **A** – the alveolar process (AP) is present between the roots (R) of the first molar. D, dentine; PL, periodontal ligament; DP, dental pulp. Bar: 300 μm. **B** - high magnification of alveolar process (AP) of the **A**. Numerous osteocytes (Ot) and some large cavities filled with bone marrow (Ma) are observed. Bar: 65 μm. **C–E** – several osteocytes (Ot) inside the lacunae are observed. The **F–H** show portions of sections subjected to silver impregnation method. Osteocytes of OVX group (**G**) exhibit scarce cytoplasmic processes (P) in comparison with the SHAM (**F**) and OVXE (**H**) groups. Bars: 11 μm. **I and J** – graphics showing the data (expressed as mean and standard deviation) of the percentage of interradicular bone area (**I**), and the number of osteocytes (**J**) per mm^2 of bone tissue. Asterisks indicate differences statistically significant ($p \leq 0.05$).

4. Discussion

Our results indicate an association between autophagy reduction and apoptosis increase in alveolar process osteocytes of estrogen-deficient rats. Conversely, estrogen replacement increased osteocyte viability by inhibiting apoptosis and maintaining autophagy in these cells, reinforcing the idea that autophagy exerts an important role in the maintenance of osteocyte survival and that the anti-apoptotic effect of estrogen is in part related to autophagy in alveolar process osteocytes.

Estrogen is a systemic hormone of crucial importance for bone remodeling homeostasis as estrogen deficiency is related to bone loss in women at menopause [23] and in animal models [30,43–45]. This hormone maintains bone homeostasis by inhibiting both excessive bone resorption by osteoclasts and osteoblast/osteocyte apoptosis [21,23].

In the present study, a significant reduction in the number of osteocytes accompanied by high incidence of cleaved caspases-3- and TUNEL-positive osteocytes was found in the alveolar process of rats from OVX groups. Meanwhile, significant differences in these parameters were not verified between OVXE and SHAM groups. These data reinforce the concept that estrogen depletion induces osteocytes apoptosis and that estrogen exerts an important role in the osteocyte survival [46–48]. The occurrence of apoptosis was confirmed by the presence of osteocytes exhibiting masses of condensed chromatin, typical ultrastructural features of cell undergoing apoptosis, as shown in several tissues [41,49,50]. In addition, the frequency of apoptotic osteocytes found in the SHAM group is similar to the average previously described in physiological condition (1%–5%) [46,47,51–53].

It has been demonstrated that osteocyte apoptosis increases over the first three weeks after the onset of estrogen depletion in long bone of ovariectomized rodents [47,51]. Here, the significant increase in the frequency of apoptotic osteocytes in the alveolar process of the OVX group in the basal period indicates that systemic depletion of estrogen induces osteocyte apoptosis at short time in alveolar process, as observed in the long bone. On the other hand, the bone area of the

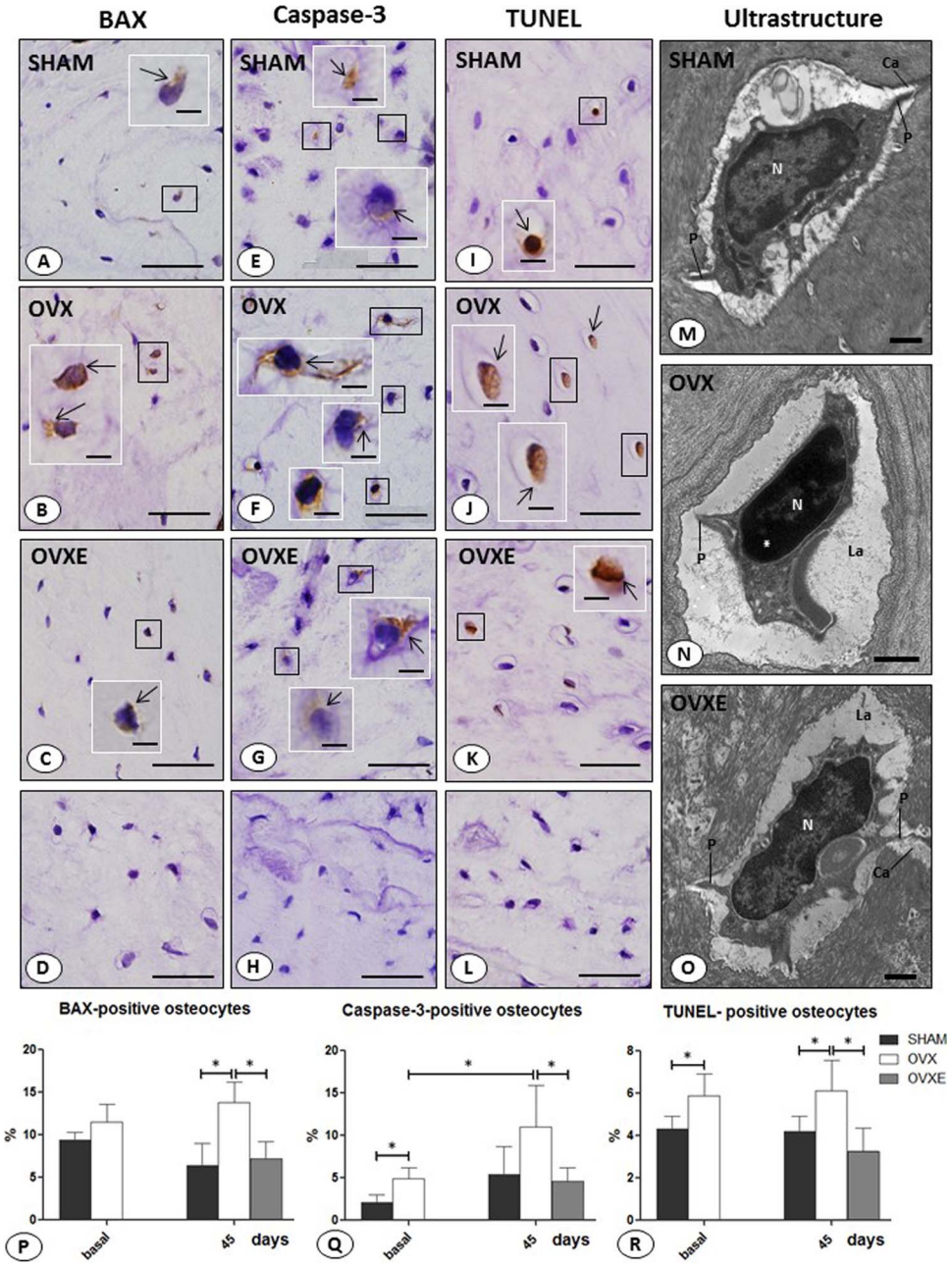

Fig. 2. A–L – Light micrographs of sections of maxilla showing portions of the interradicular alveolar process of first molars from groups at 45 days. **A–G** show portions of sections subjected to immunohistochemistry for the detection of BAX (**A–C**) or cleaved caspase-3 (**E–G**), and counterstained with hematoxylin. BAX- and caspase-3-immunostained osteocytes (brown-yellow color) are observed in all groups. The insets of the outlined areas show evident cytoplasmic immunolabeling in osteocytes (arrows). Bars: 18 μm (2A-2C); 21 μm (2E-2G); 7 μm (insets). **I–K –** sections subjected to the TUNEL method (brown-yellow color) and counterstained with hematoxylin. Scarce TUNEL-positive osteocytes (arrows) are observed in the SHAM and OVXE groups in comparison with the OVX group. Bars: 17 μm (2I-2K); 7 μm (insets). **D,H** and **L** – sections showing the negative controls of BAX (**D**), caspase-3 (**H**) and TUNEL (**L**) reactions. Note that no immunolabeled osteocytes are observed. **M–O –** Electron micrographs of portions of the alveolar process. Osteocytes within lacunae (La) show irregular and thin cytoplasmic projections (P). In the OVX group (**N**), the osteocyte exhibits a nucleus (N) which is almost completely filled by condensed chromatin (asterisk). N, nucleus; Ca, canaliculi. Bars: 1 μm. **P–R –** graphics showing the frequency (expressed as mean and standard deviation) of BAX- and caspase-3-immunolabeled osteocytes, and TUNEL-positive osteocytes. Bars with asterisks indicate differences statistically significant ($p \leq .05$).

alveolar process was significantly lower in the OVX group at the 45 days, but not in the basal period. Indeed, in this animal model it has been shown that significant ovariectomy-induced bone loss in jaw bones only occur at least 9 weeks post-surgery [30].

In different animal models, there is evidence that osteocyte apoptosis triggers the release of cytokines which stimulate the migration, differentiation and activity of osteoclasts and, consequently, bone resorption [51,54–56]. Under estrogen deficiency condition, there is an increase in osteocyte apoptosis with subsequent bone resorption by osteoclasts [53] and bone loss [52]. We observed a significant increase in the frequency of cleaved caspases-3-positive osteocytes in the OVX group at 45 days, compared with the OVX group of the basal period. This may explain, at least in part, the significant interradicular bone loss observed in the OVX group at 45 days. Our data is also in accordance with the current concept that estrogen deficiency promotes bone loss not only in the vertebrae and long bones, but in alveolar process [27,28].

The osteocyte lacuno-canalicular system plays a key role not only for the mechanosensitive function of osteocytes, but also for the supply of oxygen and nutrients to these cells [57]. It has been suggested that changes in the osteocyte communication may contribute to bone degradation during osteoporosis and reduce osteocyte viability [58]. In addition, a correlation between a reduction in osteocyte lacuno-canalicular system and an increase in the apoptosis of these cells under estrogen withdrawal has been observed [53]. In the alveolar process of rats from OVX group, the evident reduction in the presence of cytoplasmic processes of osteocytes accompanied by high incidence of apoptotic osteocytes support the concept that the interaction among osteocytes, as well as between osteocytes and osteoblasts on the bone surface is an important factor for the maintenance of osteocyte viability [57,59].

The increase in the frequency of apoptotic osteocytes in the OVX group was accompanied by a reduction in the frequency of beclin-1 and MAP LC3α-immunolabeled osteocytes, as well as with an increase in p62-positive osteocytes of OVX groups at 45 days. On the other hand, the estrogen replacement increased MAP LC3α-positive osteocytes and

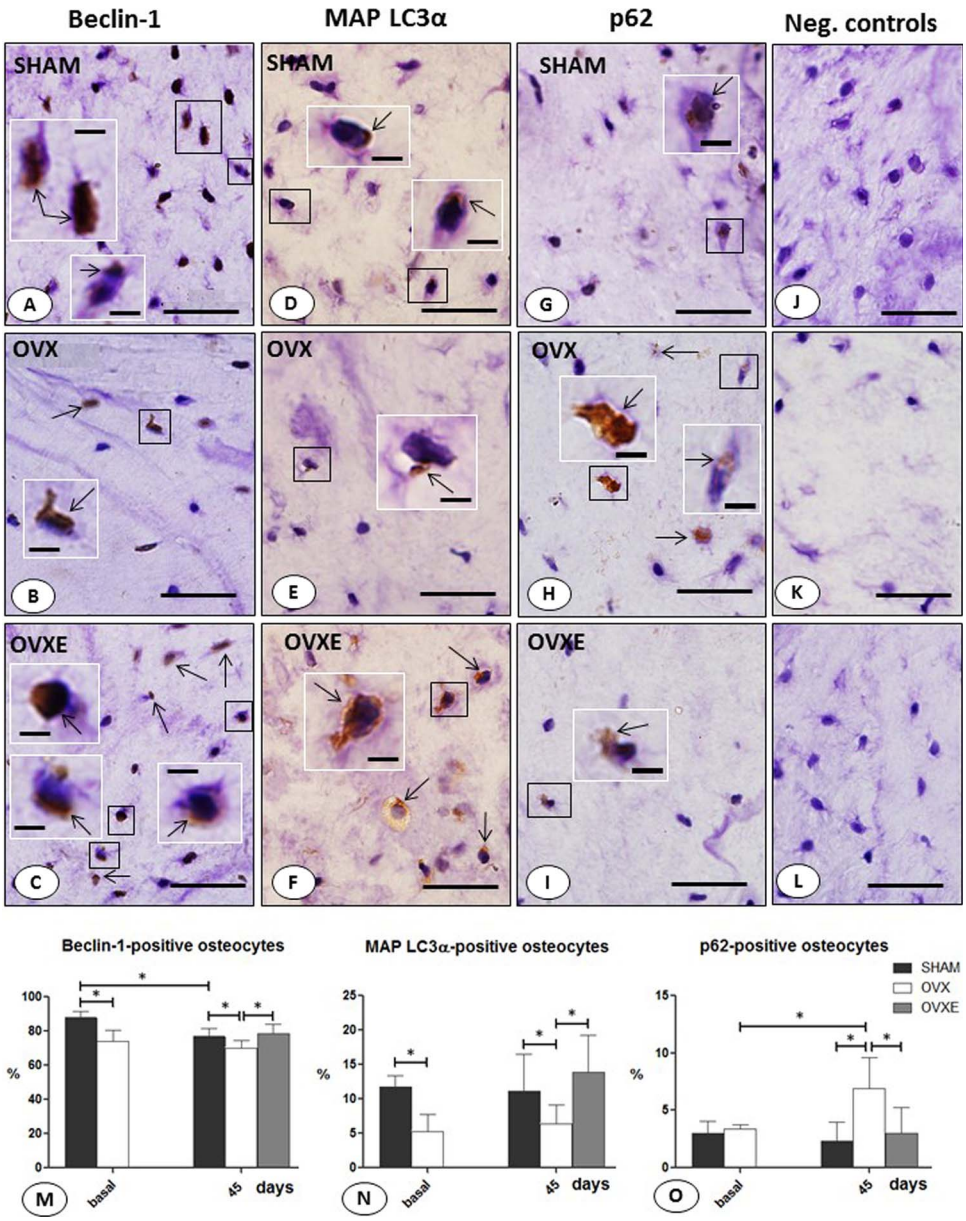

Fig. 3. A–L – Light micrographs of sections of maxilla showing portions of the interradicular alveolar process of first molars from groups at 45 days. The sections were subjected to immunohistochemistry for the detection of beclin-1 (**A–C**), MAP LC3α (**D–F**) and p62 (**G–I**) and counterstained with hematoxylin. Note the higher frequency of beclin-1- and MAP LC3α-immunolabeled osteocytes (arrows) in the SHAM (**A** and **D**) and OVXE (**C and F**), compared with the OVX group (**B** and **E**). **G–I** - osteocytes inside the lacunae exhibit p62-positive cytoplasm (arrows). **J–L** – sections showing the negative controls of beclin-1 (**J**), MAP LC3α (**K**) and p62 (**L**) immunohistochemical reactions and counterstained with hematoxylin. Note that no immunolabeled osteocytes are observed. Bars: **A–C**: 18 μm; **D–F**: 21 μm; **G–I**: 17 μm; insets: 7 μm. **M–O** – graphics showing the frequency (expressed as mean and standard deviation) of beclin-1-, MAP LC3α- and p62-immunopositive osteocytes in the bone from alveolar process. Bars and asterisks indicate differences statistically significant ($p \leq .05$).

reduced p62 immunostaining in these cells. It is known that during autophagosome formation the cytosolic form of MAP LC3-I is converted to the phosphatidylethanolamine-conjugated form (MAP LC3-II), which is recruited to the autophagosomal membrane and induces its elongation [13]. As p62 is a selective substrate of autophagosomes, and the autophagic flux activation leads to a decline in p62 expression [13], our findings strongly indicate that estrogen replacement promoted the conversion of MAP LC3I to MAP LC3II, with subsequent autophagosome formation and p62 degradation within lysosomes. In addition, these findings indicate that osteocyte apoptosis induced by estrogen depletion is associated, at least in part, to autophagy reduction in these cells, and also suggest a complex crosstalk between autophagy and apoptosis in osteocytes.

In fact, studies have indicated that there is an intricate interplay between autophagy and apoptosis pathways, whereby proteins of the apoptotic pathway participate in autophagy or *vice versa.* Under certain conditions, autophagy activation inhibits apoptosis, whereas in others apoptosis inhibits autophagy [60–63]. Indeed, it has been shown that autophagy and apoptosis communication can occur by the interaction between cleaved caspase-3 (apoptotic protein) and beclin-1 (autophagic protein). In this case, active caspase-3 can cleave beclin-1, thus inhibiting its proautophagic activity. As a result of this cleavage, the C- and N- terminal fragments of beclin-1 translocate to the mitochondria and stimulate the mitochondrial mediated apoptosis [63]. In our study, the reduction of beclin-1-immunolabeled in parallel with the increase of cleaved caspase-3-immunolabeled osteocytes is in accordance with the idea of beclin-1 cleavage by activated caspase-3 [64,65], which may be responsible for the increased apoptosis and reduced autophagy after OVX.

It has been reported that estrogen inhibits osteocytes apoptosis by acting through the ERK1/2 (extracellular signal-regulated protein kinases 1 and 2) by binding to its receptors on the cell surface [66]. ERK is one of the survival pathways that activate autophagy [32], suggesting that estrogen maintains bone cell viability by acting through autophagy pathway. Accordingly, it has been shown that estrogen inhibits osteoblast apoptosis in vitro by increasing autophagy through the estrogen receptor-ERK-mTOR pathway, whereby estrogen inhibits mTOR (mammalian target of rapamycin) phosphorylation, causing its inactivation and subsequent autophagy pathway activation in osteoblasts [67]. In the present study, the accentuated incidence of beclin-1 and

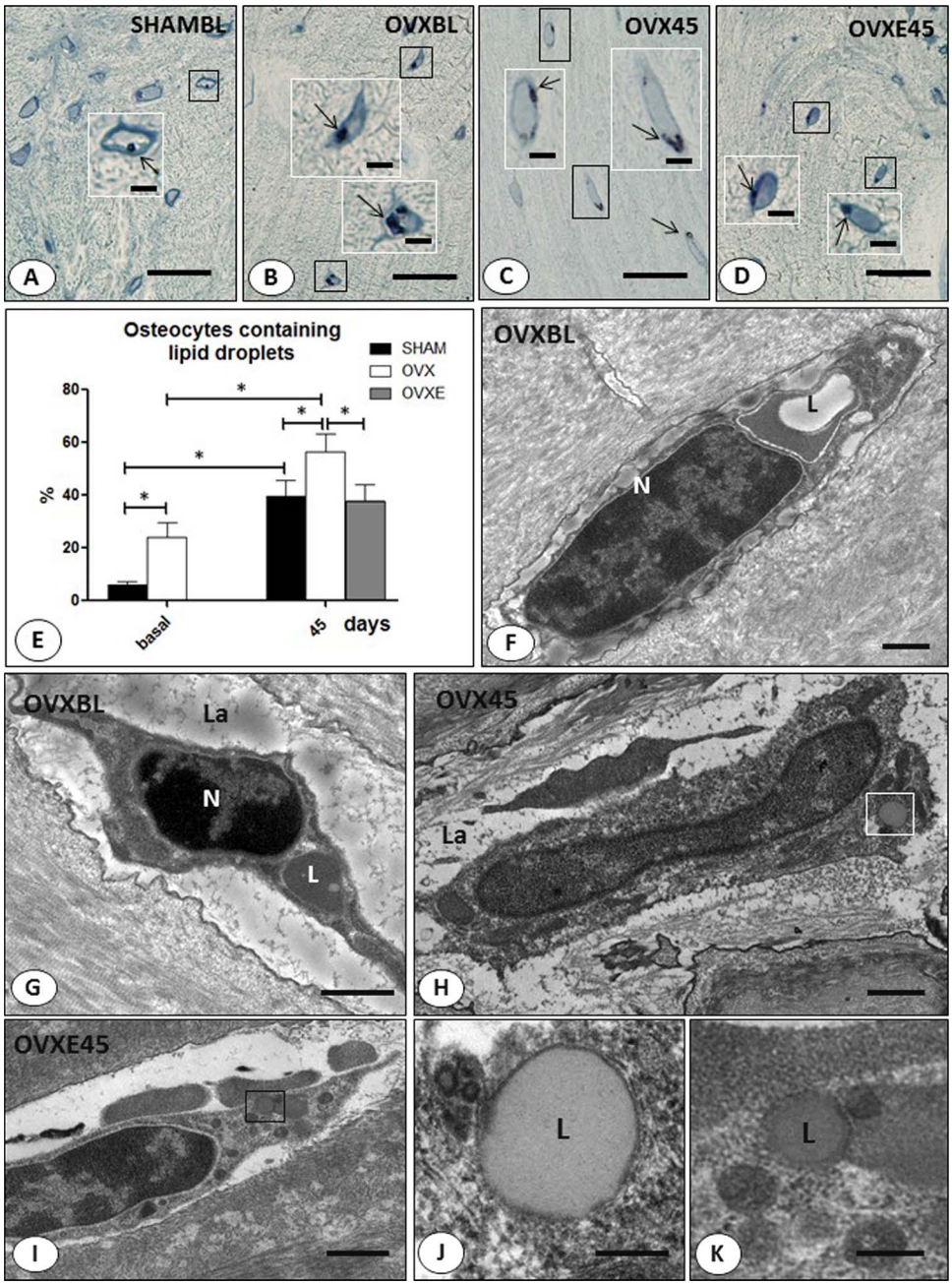

Fig. 4. A–D – Light micrographs of semithin sections of the interradicular alveolar process of first molars. The sections were subjected to the Sudan Black method and counterstained with methylene blue/azure II solution. Sudan Black structures (arrows), which indicate the presence of lipids, are observed in the cytoplasm of osteocytes of the alveolar process of all the groups. Scale bars: 18 μm and 7 μm (insets). **E** - Graphic showing the frequency (expressed as mean and standard deviation) of osteocytes containing Sudan Black structures. Bars with asterisks indicate differences statistically significant ($p \leq 0.05$). **F–K** – Electron micrographs of portions of the alveolar process. Osteocytes within lacunae (La) show lipid droplets (L) in their cytoplasm. In **G** (OVXBL), note that the osteocyte exhibits nucleus with condensed chromatin (N). **J** and **K**, higher magnifications of outlined areas in the **H** and **I**, respectively, show homogeneous and electron-opaque aspect of the lipid droplets. Scale bars: 1 μm (4F, 4G, 4H and 4I); 0.2 μm (4J); 0.25 μm (4 K).

MAP LC3α-immunolabeled osteocytes associated to the reduced number of apoptotic osteocytes in the OVXE groups indicates that estrogen may maintain osteocyte viability by activating autophagic pathways.

In contrast, estrogen deficiency and its replacement have been shown to promote, respectively, autophagy increase and its reduction in osteocytes of proximal tibias of ovariectomized rats [25]. According the authors, estrogen deficiency seems increase oxidative stress, an autophagy stimulating factor [11], in osteocytes, whereas estrogen replacement could act as an antioxidant factor and thus counteracting this effect [53]. However, it is important to mention that despite histologically similar to long bone, jaws display different responses to osteogenic, mechanical loading and homeostatic regulatory signals [30–33]. It is known that bone turnover is higher in jaw than in long bones [68]. In addition, it has been shown that jaw, vertebral and long bones respond differently to estrogen deficiency in animal models [30]. The different responses induced by hypoxia on distinct osteocyte population of cortical bone were associated to the intrinsic capacity of these cells to remove damaged mitochondria by autophagy (mitophagy) [69]. Taking all these differences into account jaws and long bones may also present different autophagy levels in response to estrogen status, which could explain, at least in part, the differences of our results from previous studies in long bone [25].

The Sudan Black-positive structures in the osteocytes indicate the presence of lipid droplets [42]. Cytoplasmic storage of lipid droplets is an important source of energy for cells when necessary [70]. However, abnormal intracellular lipid storage can cause cell and tissue damage, which is associated with several diseases [71]. In osteocytes, a strong correlation between increased lipid storage and apoptosis has been demonstrated in rat model of alcohol-induced osteopenia [72]. In the present study, the accumulation of lipid droplets in osteocytes of estrogen deficient rats may be partially associated to osteocyte apoptosis. This hypothesis is supported by the increased incidence of osteocytes containing lipid droplets in parallel with the increased frequency of

caspase-3- and TUNEL-positive osteocytes. Moreover, some osteocytes of alveolar process from OVX group containing lipid droplets exhibited condensed chromatin, typical characteristic of apoptosis [41,49,50].

It is known that lipid droplets are degraded in autophagosomes, a process called lipophagy [73]. The association between autophagy reduction and lipid droplets accumulation has been reported in different cell types [74]. Therefore, the increase in the frequency of osteocytes exhibiting lipid droplets in the OVX group may also be in part associated with autophagy reduction, since the lower frequency of osteocytes immunostained for autophagic markers was found in this group. Conversely, the high frequency of osteocytes immunostained for the autophagic markers was correlated with low number of osteocytes containing lipid droplets in the estrogen treated group. To our knowledge, this is the first evidence of a possible role of estrogen in osteocyte lipophagy.

5. Conclusion

Taken together, our results indicate that estrogen deficiency decreases autophagy and increases apoptosis in alveolar process osteocytes. On the other hand, estrogen replacement enhances osteocyte viability by inhibiting apoptosis and maintaining autophagy in these cells. These results reinforce the role of estrogen on the autophagy process and suggest that the anti-apoptotic effects of estrogen may be, at least in part, related to autophagy regulation in alveolar process osteocytes. Future studies exploring the induction/inhibition of autophagy genetically or pharmacologically will needed to be addressed in post-menopausal animal models, in order to better understand the relationship between the anti-apoptotic effects of estrogen and the autophagy pathway in osteocytes. The complete elucidation of this relationship could contribute to a better understanding of the molecular and cellular mechanisms involved in post-menopausal osteoporosis and to target new treatments.

Conflict of interest

All authors declare no conflict of interest.

Disclosures

None

Acknowledgements

The authors thank Mr Luis Antônio Potenza, Mr Pedro Sérgio Simões and Mr Paulo Celso Franco for technical assistance, and Cristiane de Paula Teixeira for the estradiol serum assay. This research was supported by public funding from São Paulo Research Foundation (FAPESP – grant numbers 2012/19428-8; 2012/22666-8), National Council for Scientific and Technological Development (CNPq) and by Coordination of Improvement of Higher Level Personnel (CAPES), Brazil.

References

[1] M.B. Schaffler, W.Y. Cheung, R. Majeska, O. Kennedy, Osteocytes: master orchestrators of bone, Calcif. Tissue Int. 94 (1) (2014) 5–24.
[2] R. Florencio-Silva, G.R.S. Sasso, E. Sasso-Cerri, M.J. Simões, P.S. Cerri, Biology of bone tissue: structure, function, and factors that influence bone cells, Biomed. Res. Int. 2015 (2015) 421746.
[3] M. Prideaux, D.M. Findlay, G.J. Atkins, Osteocytes: the master cells in bone remodeling, Curr. Opin. Pharmacol. 28 (2016) 24–30.
[4] S.C. Manolagas, A.M. Parfitt, What old means to bone, Trends Endocrinol. Metab. 21 (6) (2010) 369–374.
[5] A.M. Zahm, J. Bohensky, C.S. Adams, I.M. Shapiro, V. Srinivas, Bone cell autophagy is regulated by environmental factors, Cells Tissues Organs 194 (2–4)) (2011) 274–278.
[6] L.J. Hocking, C. Whitehouses, M.H. Helfrich, Autophagy: a new player in skeletal maintenance? J. Bone Miner. Res. 27 (7) (2012) 1439–1447.
[7] W. Yao, W. Dai, J.X. Jiang, N.E. Lane, Glucocorticoids and osteocyte autophagy, Bone 54 (2) (2013) 279–284.
[8] M. Piemontese, M. Onal, J. Xiong, L. Han, J.D. Thostenson, M. Almeida, C.A. O'Brien, Low bone mass and changes in the osteocyte network in mice lacking autophagy in the osteoblast lineage, Sci. Rep. 6 (2016) 24262.
[9] Z. Yang, D.J. Klionsky, Eaten alive: a history of macroautophagy, Nat. Cell Biol. 12 (9) (2010) 814–822.
[10] G. Filomeni, D. De Zio, F. Cecconi, Oxidative stress and autophagy: the clash between damage and metabolic needs, Cell Death Differ. 22 (3) (2015) 377–388.
[11] M.C. Maiuri, G. Kroemer, Autophagy in stress and disease, Cell Death Differ. 22 (3) (2015) 365–366.
[12] G.M. Cann, C. Guignabert, L. Ying, N. Deshpande, J.M. Bekker, L. Wang, B. Zhou, M. Rabinovitch, Developmental expression of LC3alpha and beta: absence of fibronectin or autophagy phenotype in LC3beta knockout mice, Dev. Dyn. 237 (1) (2008) 187–195.
[13] Y. Ichimura, M. Komatsu, Selective degradation of p62 by autophagy, Semin. Immunopathol. 32 (4) (2010) 431–436.
[14] I.M. Shapiro, R. Layfield, M. Lotz, C. Settembre, C. Whitehouse, Boning up on autophagy: the role of autophagy in skeletal biology, Autophagy 10 (1) (2014) 7–19.
[15] V. Pierrefite-Carle, S. Santucci-Darmanin, V. Breuil, O. Camuzard, G.F. Carle, Autophagy in bone: self-eating to stay in balance, Ageing Res. Rev. 24 (Pt. B) (2015) 206–217.
[16] R. Florencio-Silva, G.R.S. Sasso, M.J. Simões, R.S. Simões, M.C.P. Baracat, E. Sasso-Cerri, P.S. Cerri, Osteoporosis and autophagy: what is the relationship? Rev. Assoc. Med. Bras. 63 (2) (2017) 173–179.
[17] L. Zhang, Y.F. Guo, Y.Z. Liu, Y.J. Liu, D.H. Xiong, X.G. Liu, L. Wang, T.L. Yang, S.F. Lei, Y. Guo, H. Yan, Y.F. Pei, F. Zhang, C.J. Papasian, R.R. Recker, H.W. Deng, Pathway-based genome-wide association analysis identified the importance of regulation of autophagy pathway for ultradistal radius BMD, J. Bone Miner. Res. 25 (7) (2010) 1572–1580.
[18] M. Onal, M. Piemontese, J. Xiong, Y. Wang, L. Han, S. Ye, M. Komatsu, M. Selig, R.S. Weinstein, H. Zhao, R.L. Jilka, M. Almeida, S.C. Manolagas, C.A. O'Brien, Suppression of autophagy in osteocytes mimics skeletal aging, J. Biol. Chem. 288 (24) (2013) 1732–1740.
[19] K. Chen, Y.H. Yang, S.D. Jiang, L.S. Jiang, Decreased activity of osteocyte autophagy with aging may contribute to the bone loss in senile population, Histochem. Cell Biol. 142 (3) (2014) 285–295.
[20] D. Luo, H. Ren, T. Li, K. Lian, D. Lin, Rapamycin reduces severity of senile osteoporosis by activating osteocyte autophagy, Osteoporos. Int. 27 (3) (2016) 1093–1101.
[21] M. Almeida, M.R. Laurent, V. Dubois, F. Claessens, C.A. O'Brien, R. Bouillon, D. Vanderschueren, S.C. Manolagas, Estrogens and androgens in skeletal physiology and pathophysiology, Physiol. Rev. 97 (1) (2017) 135–187.
[22] M. Cruzoe-Souza, E. Sasso-Cerri, P.S. Cerri, Immunohistochemical detection of estrogen receptor beta in alveolar bone cells of estradiol-treated female rats: possible direct action of estrogen on osteoclast life span, J. Anat. 215 (2009) 673–681.
[23] S. Khosla, M.J. Oursler, D.G. Monroe, Estrogen and the skeleton, Trends Endocrinol. Metab. 23 (11) (2012) 576–581.
[24] Y.H. Yang, K. Chen, B. Li, J.W. Chen, X.F. Zheng, Y.R. Wang, S.D. Jiang, L.S. Jiang, Estradiol inhibits osteoblast apoptosis via promotion of autophagy through the ER-ERK-mTOR pathway, Apoptosis 18 (11) (2013) 1363–1375.
[25] Y. Yang, X. Zheng, B. Li, S. Jiang, L. Jiang, Increased activity of osteocyte autophagy in ovariectomized rats and its correlation with oxidative stress status and bone loss, Biochem. Biophys. Res. Commun. 451 (1) (2014) 86–92.
[26] M. Tanaka, S. Ejiri, E. Toyooka, S. Kohno, H. Ozawa, Effects of ovariectomy on trabecular structures of rat alveolar bone, J. Periodontal Res. 37 (2) (2002) 161–165.
[27] F.E. FArdakani, S.J. Mirmohamadi, Osteoporosis and oral bone resorption: a review, J. Maxillofac. Oral Surg. 8 (2) (2009) 121–126.
[28] R. Guiglia, O. Di-Fede, L. Lo-Russo, D. Sprini, G.B. Rini, G. Campisi, Osteoporosis, jawbones and periodontal disease, Med. Oral. Patol. Oral Cir. Bucal 18 (1) (2013) e93–e99.
[29] X.C. Xu, H. Chen, X. Zhang, Z.J. Zhai, X.Q. Liu, X.Y. Zheng, J. Zhang, A. Qin, E.Y. Lu, Effects of oestrogen deficiency on the alveolar bone of rats with experimental periodontitis, Mol. Med. Rep. 12 (3) (2015) 3494–3502.
[30] B.D. Johnston, W.E. Ward, The ovariectomized rat as a model for studying alveolar bone loss in postmenopausal women, Biomed. Res. Int. 2015 (2015) 635023.
[31] T.L. Aghaloo, T. Chaichanasakul, O. Bezouglaia, B. Kang, R. Franco, S.M. Dry, E. Atti, S. Tetradis, Osteogenic potential of mandibular vs. long-bone marrow stromal cells, J. Dent. Res. 89 (11) (2010) 1293–1298.
[32] A.P. de Souza Faloni, T. Schoenmaker, A. Azari, E. Katchburian, P.S. Cerri, T.J. de Vries, V. Everts, Jaw and long bone marrows have a different osteoclastogenic potential, Calcif. Tissue Int. 88 (1) (2011) 63–74.
[33] T. Matsuura, K. Tokutomi, M. Sasaki, M. Katafuchi, E. Mizumachi, H. Sato, Distinct characteristics of mandibular bone collagen relative to long bone collagen: relevance to clinical dentistry, Biomed. Res. Int. 2014 (2014) 769414.
[34] S. Oestergaard, B.C. Sondergaard, P. Hoegh-Andersen, K. Henriksen, P. Qvist, C. Christiansen, L.B. Tankó, M.A. Karsdal, Effects of ovariectomy and estrogen therapy on type II collagen degradation and structural integrity of articular cartilage in rats: implications of the time of initiation, Arthritis Rheum. 54 (8) (2006) 2441–2451.
[35] S.E. Lin, J.P. Huang, L.Z. Wu, T. Wu, L. Cui, Prevention of osteopenia and dyslipidemia in rats after ovariectomy with combined aspirin and low-dose diethylstilbestrol, Biomed. Environ. Sci. 26 (4) (2013) 249–257.
[36] D.W. Dempster, J.E. Compston, M.K. Drezner, F.H. Glorieux, J.A. Kanis, H. Malluche, P.J. Meunier, S.M. Ott, R.R. Recker, A.M. Parfitt, Standardized

nomenclature, symbols, and units for bone histomorphometry: a 2012 update of the report of the ASBMR histomorphometry nomenclature committee, J. Bone Miner. Res. 28 (1) (2013) 2–17.
[37] N.M. Ocarino, M.G. Gomes, E.G. Melo, R. Serakides, Técnica histoquímica aplicada ao tecido ósseo desmineralizado e parafinado para o estudo do osteócito e suas conexões, J. Bras. Patol. Med. Lab. 42 (1) (2006) 37–39.
[38] Y. Gavrieli, Y. Sherman, S.A. Ben-Sasson, Identification of programmed cell death in situ via specific labeling of nuclear DNA fragmentation, J. Cell Biol. 119 (3) (1992) 493–501.
[39] P.S. Cerri, Osteoblasts engulf apoptotic bodies during alveolar bone formation in the rat maxilla, Anat. Rec. 286 (1) (2005) 833–840.
[40] D.J. Klionsky, K. Abdelmohsen, A. Abe, et al., Guidelines for the use and interpretation of assays for monitoring autophagy, Autophagy 12 (1) (2012) 1–222 (2016).
[41] R. Longhini, P.A. de Oliveira, A.P. de Souza Faloni, E. Sasso-Cerri, P.S. Cerri, Increased apoptosis in osteoclasts and decreased RANKL immunoexpression in periodontium of cimetidine-treated rats, J. Anat. 222 (2) (2013) 239–247.
[42] J.A. Kiernan, Histological and Histochemical Methods: Theory and Practice, fourth ed., Scion Publishing, Oxford, 2008.
[43] J. Fox, M.K. Newman, C.H. Turner, R.E. Guldberg, A. Varela, S.Y. Smith, Effects of treatment with parathyroid hormone 1-84 on quantity and biomechanical properties of thoracic vertebral trabecular bone in ovariectomized rhesus monkeys, Calcif. Tissue Int. 82 (3) (2008) 212–220.
[44] D. Choudhary, P. Kushwaha, J. Gautam, P. Kumar, A. Verma, A. Kumar, S.W. Maurya, I.R. Siddiqui, P.R. Mishra, R. Maurya, R. Trivedi, Fast and long acting neoflavonoids dalbergin isolated from Dalbergia sissoo heartwood is osteoprotective in ovariectomized model of osteoporosis: osteoprotective effect of dalbergin, Biomed. Pharmacother. 83 (2016) 942–957.
[45] H.M. Abuohashish, M.M. Ahmed, D. Sabry, M.M. Khattab, S.S. Al-Rejaie, ACE-2/Ang1-7/Mas cascade mediates ACE inhibitor, captopril, protective effects in estrogen-deficient osteoporotic rats, Biomed. Pharmacother. 92 (2017) 58–68.
[46] A. Tomkinson, J. Reeve, R.W. Shaw, B.S. Noble, The death of osteocytes via apoptosis accompanies estrogen withdrawal in human bone, J. Clin. Endocrinol. Metab. 82 (9) (1997) 3128–3135.
[47] A. Tomkinson, E.F. Gevers, J.M. Wit, J. Reeve, B.S. Noble, The role of estrogen in the control of rat osteocyte apoptosis, J. Bone Miner. Res. 13 (8) (1998) 1243–1250.
[48] N. Marathe, H. Rangaswami, S. Zhuang, G.R. Boss, R.B. Pilz, Pro-survival effects of 17-estradiol on osteocytes are mediated by nitric oxide/cGMP via differential actions of cGMP-dependent protein kinases I and II, J. Biol. Chem. 287 (2) (2012) 978–988.
[49] B.H. Caneguim, P.S. Cerri, L.C. Spolidório, S.M. Miraglia, E. Sasso-Cerri, Immunosuppressant Prograf® (tacrolimus) induces histopathological disorders in the peritubular tissue of rat testes, Cells Tissues Organs 194 (5) (2011) 421–430.
[50] J.P. de Pizzol Júnior, E. Sasso-Cerri, P.S. Cerri, Apoptosis and reduced microvascular density of the lamina propria during tooth eruption in rats, J. Anat. 227 (4) (2015) 487–496.
[51] K.B. Emerton, B. Hu, A.A. Woo, A. Sinofsky, C. Hernandez, R.J. Majeska, K.J. Jepsen, M.B. Schaffler, Osteocyte apoptosis and control of bone resorption following ovariectomy in mice, Bone 46 (3) (2010) 577–583.
[52] R.L. Jilka, B. Noble, R.S. Weinstein, Osteocyte apoptosis, Bone 54 (2) (2013) 264–271.
[53] M. Almeida, L. Han, M. Martin-Millan, L.I. Plotkin, S.A. Stewart, P.K. Roberson, S. Kousteni, C.A. O'Brien, T. Bellido, A.M. Parfitt, R.S. Weinstein, R.L. Jilka, S.C. Manolagas, Skeletal involution by age-associated oxidative stress and its acceleration by loss of sex steroids, J. Biol. Chem. 282 (37) (2007) 27285–27297.
[54] O.D. Kennedy, D.M. Laudier, R.J. Majeska, H.B. Sun, M.B. Schaffler, Osteocyte apoptosis is required for production of osteoclastogenic signals following bone fatigue in vivo, Bone 64 (2014) 132–137.
[55] L.I. Plotkin, Apoptotic osteocytes and the control of targeted bone resorption, Curr. Osteoporos. Rep. 12 (1) (2014) 121–126.
[56] P. Cabahug-Zuckerman, D. Frikha-Benayed, R.J. Majeska, A. Tuthill, S. Yakar, S. Judex, M.B. Schaffler, Osteocyteosteocyte apoptosis caused by hindlimb unloading is required to trigger osteocyte RANKL production and subsequent resorption of cortical and trabecular bone in mice femurs, J. Bone Miner. Res. 31 (7) (2016) 1356–1365.
[57] S.L. Dallas, M. Prideaux, L.F. Bonewald, The osteocyte: an endocrine cell ... and more, Endocr. Rev. 34 (5) (2013) 658–690.
[58] D. Sharma, C. Ciani, P.A. Marin, J.D. Levy, S.B. Doty, S.P. Fritton, Alterations in the osteocyte lacunar-canalicular microenvironment due to estrogen deficiency, Bone 51 (3) (2012) 488–497.
[59] T. Komori, Functions of the osteocyte network in the regulation of bone mass, Cell Tissue Res. 352 (2) (2013) 191–198.
[60] G.M. Fimia, M. Piacentini, Regulation of autophagy in mammals and its interplay with apoptosis, Cell. Mol. Life. Sci. 67 (10) (2010) 1581–1588.
[61] S. Mukhopadhyay, P.K. Panda, N. Sinha, D.N. Das, S.K. Bhutia, Autophagy and apoptosis: where do they meet? Apoptosis 19 (4) (2014) 555–566.
[62] G. Mariño, M. Niso-Santano, E.H. Baehrecke, G. Kroemer, Self-consumption: the interplay of autophagy and apoptosis, Nat. Rev. Mol. Cell Biol. 15 (2) (2014) 81–94.
[63] M. Li, P. Gao, J. Zhang, Crosstalk between autophagy and apoptosis: potential and emerging therapeutic targets for cardiac diseases, Int. J. Mol. Sci. 17 (3) (2016) 332.
[64] E. Wirawan, L. Vande Walle, K. Kersse, S. Cornelis, S. Claerhout, I. Vanoverberghe, R. Roelandt, R. De Rycke, J. Verspurten, W. Declercq, P. Agostinis, T. Vanden Berghe, S. Lippens, P. Vandenabeele, Caspase-mediated cleavage of beclin-1 inactivates beclin-1-induced autophagy and enhances apoptosis by promoting the release of proapoptotic factors from mitochondria, Cell Death Dis. 1 (e18) (2010), http://dx.doi.org/10.1038/cddis.2009.16.
[65] Y. Zhu, L. Zhao, L. Liu, P. Gao, W. Tian, X. Wang, H. Jin, H. Xu, Q. Chen, Beclin 1 cleavage by caspase-3 inactivates autophagy and promotes apoptosis, Protein Cell 1 (5) (2010) 468–477.
[66] S. Kousteni, T. Bellido, L.I. Plotkin, C.A. O'Brien, D.L. Bodenner, L. Han, K. Han, G.B. DiGregorio, J.A. Katzenellenbogen, B.S. Katzenellenbogen, P.K. Roberson, R.S. Weinstein, R.L. Jilka, S.C. Manolagas, Nongenotropic, sex-nonspecific signaling through the estrogen or androgen receptors. Dissociation from transcriptional activity, Cell 104 (5) (2001) 719–730.
[67] C. He, D. Klionsky, Regulation mechanisms and signaling pathways of autophagy, Annu. Rev. Genet. 43 (2009) 67–93.
[68] S.S. Huja, S.A. Fernandez, K.J. Hill, Y. Li, Remodeling dynamics in the alveolar process in skeletally mature dogs, Anat. Rec. A. Discov. Mol. Cell. Evol. Biol. 288 (12) (2006) 1243–1249.
[69] D. Frikha-Benayed, J. Basta-Pljakic, R.J. Majeska, M.B. Schaffler, Regional differences in oxidative metabolism and mitochondrial activity among cortical bone osteocytes, Bone 90 (2016) 15–22.
[70] Y. Guo, K.R. Cordes, R.V. Farese Jr, T.C. Walther, Lipid droplets at a glance, J. Cell Sci. 122 (Pt6) (2009) 749–752.
[71] R.V. Farese, T.C. Walther, Lipid droplets finally get a little R-E-S-P-E-C-T, Cell 139 (5) (2009) 855–860.
[72] D.B. Maurel, D. Benaitreau, C. Jaffré, H. Toumi, H. Portier, R. Uzbekov, C. Pichon, C.L. Benhamou, E. Lespessailles, S. Pallu, Effect of the alcohol consumption on osteocyte cell processes: a molecular imaging study, J. Cell. Mol. Med. 18 (8) (2014) 1680–1693.
[73] R. Singh, S. Kaushik, Y. Wang, Y. Xiang, I. Novak, M. Komatsu, K. Tanaka, A.M. Cuervo, M.J. Czaja, Autophagy regulates lipid metabolism, Nature 458 (7242) (2009) 1131–1135.
[74] H. Dong, M.J. Czaja, Regulation of lipid droplets by autophagy, Trends Endocrinol. Metab. 22 (6) (2011) 234–240.